Enhancing Effect of Residual Capping Agents in Heterogeneous Enantioselective Hydrogenation of α-keto Esters over Polymer-Capped Pt/Al₂O₃

Iljun Chung,[†] Byeongju Song,[†] Jeongmyeong Kim, and Yongju Yun*

Read Online

ACCESS | Metrics & More | Article Recommendations | SI Supporting Information

ABSTRACT: Heterogeneous enantioselective catalysis is considered a promising strategy for the large-scale production of enantiopure chemicals. In this work, polymer-capped Pt nanocatalysts having a uniform size were synthesized using poly(vinyl pyrrolidone) (PVP) and poly(vinyl alcohol) and supported on γ-Al₂O₃. After a facile heat treatment process, their catalytic performance for enantioselective hydrogenation of α-keto esters, a structure-sensitive reaction, was investigated. The presence of residual capping agents on the Pt surface often perturbs the adsorption of reacting species and reduces performance in structure-sensitive reactions. However, the 1 wt % PVP-Pt/Al₂O₃ catalyst exhibited an enhancement in both activity and enantioselectivity compared to a reference Pt/Al₂O₃ catalyst prepared by wet impregnation. Under optimized reaction conditions, the cinchonidine-modified PVP-Pt/Al₂O₃ gave an enantiomeric excess of 95% for the enantioselective hydrogenation of methyl pyruvate despite the low Pt loading. We demonstrate that depending on the type of polymers, the residual capping agents can lead to site-selective blockage of the Pt surface, that is, defects or terraces. Quantitative and qualitative analyses also show that the noticeable improvement in enantioselectivity is attributed to the stable adsorption of chiral modifiers on selectively exposed Pt terrace sites. The findings of this work provide a promising strategy to prepare metal nanoparticles having selectively exposed sites and offer insights into the enhancing effect of residual capping agents on the catalytic properties in structure-sensitive reactions.

KEYWORDS: heterogeneous, enantioselective, hydrogenation, nanocatalyst, capping agent

Heterogeneous enantioselective hydrogenation

α-keto ester → CD or QN, H₂ / AcOH → (R)-hydroxy ester

PVP-capped Pt/Al₂O₃ — Heat treatment — Selective exposure of "terraces" — Superior enantioselectivity

VS

PVA-capped Pt/Al₂O₃ — Selective exposure of "defects" — Inferior enantioselectivity
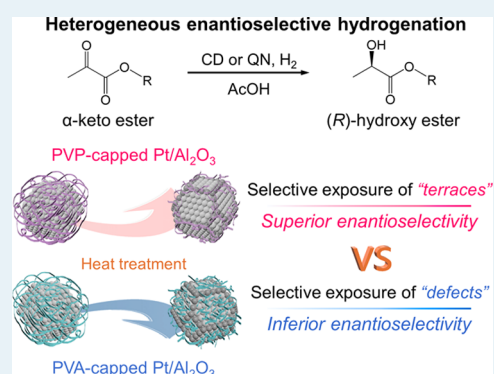
1. INTRODUCTION

Chiral molecules are key compounds in the fine chemical industry, especially for the production of pharmaceuticals, agrochemicals, and perfumes.[1,2] Crucially, the two enantiomers of a chiral molecule can have distinctly different physiological effects on the human body because of the homochirality of living organisms.[3,4] Thus, many efforts have been devoted to the production of enantiomerically pure compounds. Enantio-selective catalysis over heterogeneous catalysts is considered to be a promising strategy for the large-scale production of enantiopure chemicals because of the easy separation of the products from the catalyst and the high reusability of the catalyst.[5−7] Orito reaction, the enantioselective hydrogenation of α-keto esters over supported Pt catalysts, is a well-known example of enantioselective heterogeneous catalysis.[8] To create chirally active sites, the achiral Pt surface is modified by the adsorption of organic chiral molecules. Cinchona alkaloid-modified Pt/Al₂O₃ catalysts are an extensively studied model system because of their high enantioselectivities in which the steric hindrance by the chiral modifier leads to enantiodiffer-entiation of the complex of the modifier with the substrate on the Pt surface.[9,10]

Cinchona alkaloids, including cinchonidine (CD) and quinine (QN), are bulky chiral molecules and their quinoline rings act as anchoring moieties on the Pt surface. The enantioselective hydrogenation of α-keto esters is structure sensitive because the adsorption of the chiral modifier significantly depends on the size and surface structure of Pt nanoparticles (NPs).[11,12] The adsorbed cinchona alkaloids are stabilized on terrace sites via $\pi-\pi$ interactions between the quinoline ring and the Pt surface, resulting in a flat adsorption mode.[13] It has also been suggested that sufficient Pt sites are required to accommodate the bulky complex of the chiral modifier and the substrate.[12] Indeed, several studies have shown that Pt NPs with average sizes of less than 2 nm, which are expected to expose a large fraction of defect sites, exhibit

poor enantioselectivity.[14,15] These observations imply that the coordination of specific surface sites significantly affects the catalytic performance and that chiral modifiers adsorbed on terraces are more efficient for enantiodifferentiation than those adsorbed on defects such as steps and kinks.

Recently, the structure sensitivity of enantioselective hydrogenation has been studied using metal NPs capped with polymers such as poly(vinyl pyrrolidone) (PVP) and poly-(acrylic acid) (PAA).[11,16,17] Capping agents control the size and shape of NPs by preventing aggregation and directing the growth of particles. In many cases, however, the capping agents have adverse effects on catalytic performance because they block the active sites and, thus, hamper the adsorption of reacting species on the surface.[11,17−19] Investigation of the enantioselective hydrogenation of ethyl pyruvate (EtPy) over PAA-capped Pt NPs, modified with CD and QN, has revealed that the presence of PAA on the Pt surface leads to a loss of catalytic activity and enantioselectivity.[11] However, the partial removal of the capping agent from the Pt surface under reaction conditions results in an increase in enantioselectivity. A similar detrimental effect of the capping agent on enantioselectivity has also been observed for PVP-capped Pd NPs, modified with S-proline, in the enantioselective hydrogenation of acetophenone.[17] After the partial removal of PVP from the Pd surface by KBH$_4$ treatment or hot water reflux, the Pd catalyst showed improved enantioselectivity. These findings clearly show the importance of understanding the role of residual species on the metal surfaces in the development of nanocatalysts for heterogeneous enantioselective catalysis.

In this work, we prepared polymer-capped Pt NPs with a uniform size by using PVP and poly(vinyl alcohol) (PVA) as capping agents. After supporting the Pt NPs on γ-Al$_2$O$_3$, the Pt catalysts were heat-treated to remove the capping agents. The heat-treated Pt/Al$_2$O$_3$ contained residual capping agents on the Pt surface. In the presence of chiral modifiers, CD and QN, the catalytic performance of PVP- and PVA-Pt/Al$_2$O$_3$ catalysts with residual capping agents was investigated for the enantioselective hydrogenation of α-keto esters and compared with that of a reference catalyst with a clean Pt surface (Scheme 1). Quantitative and qualitative analyses demon-

Scheme 1. Enantioselective Hydrogenation of α-keto Esters over Chirally Modified Pt/Al$_2$O$_3$ Catalysts
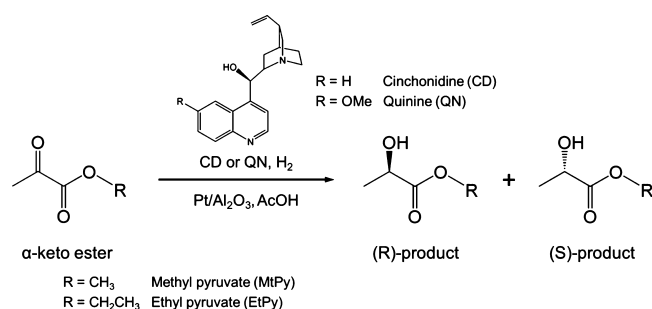
strated that the residual capping agents can selectively block the Pt sites, leaving terraces or defects exclusively exposed. Furthermore, the specific exposure of terraces led to a remarkable enhancement in the catalytic performance in the enantioselective hydrogenation of α-keto esters by enabling the stable adsorption of the chiral modifier on the Pt surface. This work offers a new strategy to prepare nanocatalysts with selectively exposed sites and shows their application in structure-sensitive reactions.

2. EXPERIMENTAL SECTION

2.1. Chemicals and Materials. For the preparation of the Pt catalysts, the following Pt precursors, capping agents, and support materials were used as received: chloroplatinic acid hydrate (H$_2$PtCl$_6$, >99.9%, Sigma-Aldrich), potassium tetrachloroplatinate (K$_2$PtCl$_4$, >99.9%, Sigma-Aldrich), platinum acetylacetonate [Pt(acac)$_2$, 98%, Acros], PVP (M_w = 55,000, Sigma-Aldrich), PVA (M_w = 31,000−50,000, Acros), and γ-Al$_2$O$_3$ support (PURALOX SCCa 5-150, S_{BET} = 169 m^2/g, Sasol). Ethylene glycol (99.8%, Sigma-Aldrich), ethanol (99.9%, Samchun Pure Chemical), acetone (99.5%, Samchun Pure Chemical), and n-hexane (95.0%, Samchun Pure Chemical) were used as solvents in the synthesis and washing procedures. For enantioselective hydrogenation, EtPy (98.0%, Alfa Aesar) and methyl pyruvate (MtPy, >97%, TCI) were used as reactants. CD (96%, Sigma-Aldrich) and QN (98%, Sigma-Aldrich) were used as chiral modifiers. The reaction was conducted in acetic acid (AcOH, 99.7%, Samchun Pure Chemical).

2.2. Preparation of Polymer-Capped Pt NPs and Supported Pt Catalysts. PVP-capped Pt NPs having an average particle size of 3 nm were synthesized by the following procedure. The Pt precursor, H$_2$PtCl$_6$ (0.1 mmol), and PVP (0.004 mmol) were added to ethylene glycol (20 mL) in a 100 mL three-neck flask, and the solution was placed under vacuum for 30 min for degassing. Then, the solution was heated at 483 K for 10 min under an Ar atmosphere. The synthesized PVP-Pt NPs were then precipitated in the presence of excess acetone by centrifugation. Excess PVP on the Pt NPs was removed by the repeated suspension of Pt NPs in ethanol and precipitation with hexane. The washed PVP-Pt NPs were finally dispersed in ethanol. The PVA-capped Pt NPs having an average particle size of 3 nm were prepared by the following procedure. PVA (0.006 mmol) was added to deionized H$_2$O (20 mL), and the mixture was heated at 373 K for 1 h. After the dissolution of K$_2$PtCl$_4$ (0.06 mmol) in the solution, it was heated at 333 K for 20 min.

Supported Pt catalysts were prepared by the following procedure. A powder of γ-Al$_2$O$_3$ was added to the solution containing the synthesized polymer-capped Pt NPs. Then, the solvent containing PVP-Pt or PVA-Pt NPs was evaporated by stirring the solution overnight at 313 or 328 K, respectively. The obtained powder was dried at 353 K for 12 h in an oven and then calcined at 623 K for 10 min to remove the capping agents. As a reference catalyst, a supported Pt catalyst without a capping agent (IMP-Pt/Al$_2$O$_3$) was prepared using the wet impregnation method. Pt(acac)$_2$ (0.064 mmol) was dissolved in acetone (20 mL). Then, an adequate amount of γ-Al$_2$O$_3$ was added to the solution, and the mixture was stirred overnight at 313 K. The obtained powder was dried at 383 K for 12 h and calcined at 623 K for 3 h under Ar flow.

2.3. Characterization of Pt NPs and Supported Pt Catalysts. Transmission electron microscopy (TEM) images were obtained using a JEOL JEM-2100F FE-TEM at an acceleration voltage of 200 kV at the National Institute for Nanomaterials Technology, Pohang, South Korea. Thermogravimetric analysis (TGA) was carried out on a HITACHI STA 7300 instrument. Samples (30 mg) were charged into the sample pan and then heated to 1000 K at a heating rate of 5 K/min in flowing air (200 sccm). The Pt loading was determined
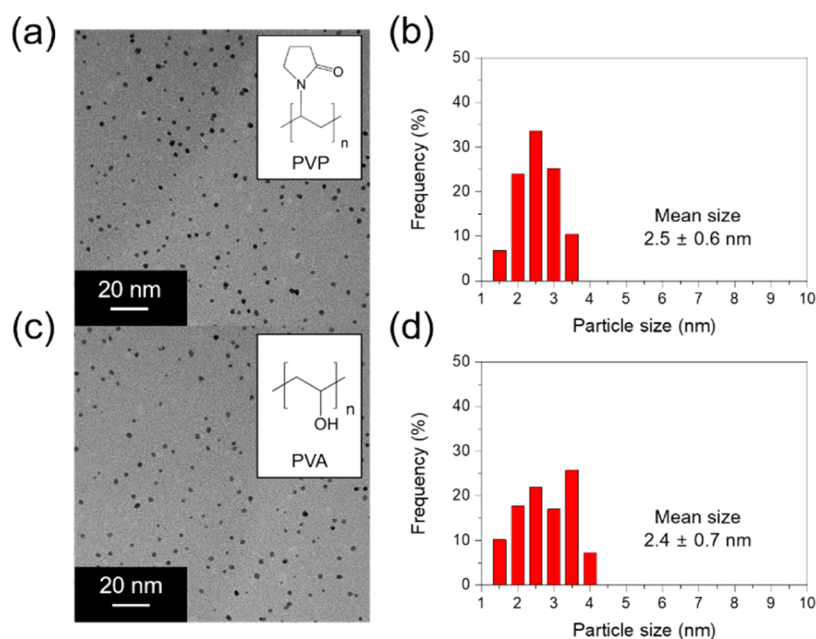
Figure 1. TEM images and size distribution histograms of as-prepared (a,b) PVP-Pt and (c,d) PVA-Pt. Both PVP-Pt and PVA-Pt NPs have uniform sizes of 2−3 nm.

by inductively coupled plasma-optical emission spectroscopy (ICP-OES) on a Thermo Scientific model iCAP 6300 spectrometer. The amount of CO chemisorbed on the Pt catalysts was determined by the CO pulse chemisorption technique using a MicrotracBEL BELCAT-II. The metal dispersion and particle sizes were calculated from the amount of chemisorbed CO on the Pt catalysts using the following equations: by assuming a CO/Pt adsorption stoichiometry of 1. The metal dispersion (D) and particle size (d) were calculated using the following equations[20,21]

$$D[\%] = \frac{V_{CO} \times SF \times MW}{W_{Pt} \times 22414} \times 100 \qquad (1)$$

$$d[nm] = \frac{600 \times MW}{D \times N_a \times \rho \times \sigma} \qquad (2)$$

where V_{CO} is the volume of the adsorbed CO [cm^3], SF is the stoichiometry factor, 1 for CO chemisorption on Pt, MW is the atomic weight of the Pt [g/mol], W_{Pt} is the weight of supported Pt on the sample [g], D is the metal dispersion [%], N_a is the Avogadro constant, ρ is the Pt metal density [g/cm^3], and σ is the cross-sectional area of one Pt atom [nm^2]. X-ray photoelectron spectroscopy (XPS) analysis was performed with a monochromatic Al Kα X-ray source ($h\nu$ = 1486.6 eV) under ultra-high vacuum at the Korea Basic Science Institute, Busan, South Korea. The binding energies were referenced to the C 1s peak at 284.6 eV. Fourier transform infrared (FTIR) transmittance spectra and diffuse reflectance Fourier transform (DRIFT) spectra were obtained with a Thermo Fisher Nicolet iS50. Sample measurements for the chemisorption of CO were carried out in an adsorption cell (PIKE Technologies DiffuseIR). The FTIR spectra were obtained from 400 to 4000 cm^{-1} using 32 scans at a spectral resolution of 4 cm^{-1} at 298 K. For DRIFT analysis of CO on Pt catalysts, the samples were reduced at 673 K under 5% H$_2$/Ar flow for 90 min and cooled to 323 K to allow the adsorption of CO. The

measurements were conducted after the samples had been purged with Ar for 5 min to remove the gaseous CO species.

2.4. Catalytic Performance Tests. The performance of the Pt catalysts was evaluated under 0.1 MPa H$_2$ pressure using a 50 mL glass reactor. For reactions at 5.0 MPa H$_2$ pressure, a stainless-steel autoclave equipped with a 100 mL glass liner was used. All catalysts were pretreated in a flow of 5% H$_2$/Ar at 673 K for 90 min. The reaction was conducted with a Pt catalyst (80 mg), a chiral modifier (6 mg), and the substrate (0.1 mL) in acetic acid (10 mL) at 298 K. Details of the procedures have been given in previous works.[22,23] The compositions of the reactant and chiral products in the solvent were analyzed by a gas chromatograph (YL6500) equipped with a Chirasil-Dex CB column (CP7502, Agilent). Turnover frequencies (TOFs) [h^{-1}] were measured based on the number of surface Pt atoms determined by CO chemisorption for IMP-Pt/Al$_2$O$_3$ and based on the number of surface Pt atoms predicted by the theoretical Pt NP model with average particle size of 3 nm for PVP- and PVA-Pt/Al$_2$O$_3$.[24−27] The enantiomeric excess (ee) of the chiral products was calculated as follows: ee [%] = |[R] − [S]|/([R] + [S]) × 100, where [R] and [S] are the concentrations of (R)- and (S)-product, respectively. The standard deviation of repeatability for conversion and enantioselectivity was less than 2.3 and 1.4%, respectively. The standard deviation of reproducibility for conversion and enantioselectivity was less than 3.4 and 1.7%, respectively.

3. RESULTS AND DISCUSSION

3.1. Preparation and Characterization of Pt/Al$_2$O$_3$ Catalysts. Enantioselective hydrogenation of α-keto esters over a Pt surface is structure sensitive because the adsorption stability and enantiodifferentiation ability of the chiral modifier are affected by the type of adsorption sites on the Pt surface.[9,28] Thus, both the reaction rate and enantioselectivity strongly depend on the size of the Pt NPs and the exposed Pt sites.[11,12,29] To exclude size effects on the catalytic performance, Pt NPs of uniform size were synthesized using two different capping agents, PVP and PVA. TEM images of the Pt

NPs capped with PVP (PVP−Pt) and PVA (PVA-Pt) and their size distributions are presented in Figure 1. The particles have narrow size distributions and mean diameters of 2−3 nm.

PVP- and PVA-Pt were deposited on γ-Al$_2$O$_3$ supports to yield the 1 wt % Pt/Al$_2$O$_3$ catalysts, denoted as PVP-Pt/Al$_2$O$_3$ and PVA-Pt/Al$_2$O$_3$, respectively. As a reference sample, 1 wt % Pt/Al$_2$O$_3$ without a capping agent, IMP-Pt/Al$_2$O$_3$, was prepared by the conventional wet impregnation method. Although capping agents are useful for the size control of NPs, the adsorbed capping agents on the metal surface can block the active sites, significantly decreasing the catalytic performance of the nanocatalysts.[11,17−19] Thus, remaining capping agents on the surface are removed by thermal treatment in air.[30,31] Before the heat treatment of PVP- and PVA-Pt/Al$_2$O$_3$, the optimal temperature was determined by TGA (Figure 2). The TGA profile of PVP-Pt/Al$_2$O$_3$ contains a
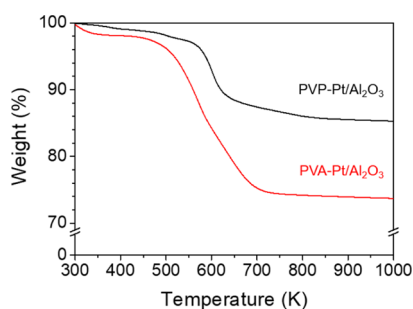
Figure 2. TGA profiles of PVP-Pt/Al$_2$O$_3$ and PVA-Pt/Al$_2$O$_3$ under continuous air flow. This shows that the optimal temperature for the removal of the capping agents from the Pt/Al$_2$O$_3$ catalysts is approximately 623 K.

sharp weight loss of 9%, originating from the thermal decomposition of PVP between 550 and 650 K. In contrast, the TGA profile of PVA-Pt/Al$_2$O$_3$ shows a weight loss of 21% over a broad range of 500−700 K. The greater weight loss of PVA-Pt/Al$_2$O$_3$ is indicative of the lower thermal stability of PVA than that of PVP, as reported previously.[32,33] On the basis of the TGA results, both PVP- and PVA-Pt/Al$_2$O$_3$ were heat-treated at 623 K in air.

Heat treatment to remove the capping agent can result in the aggregation of the Pt NPs under inappropriate conditions. Thus, after the heat treatment, the size distributions of the Pt NPs of PVP- and PVA-Pt/Al$_2$O$_3$ were confirmed again and compared with that of IMP-Pt/Al$_2$O$_3$ (Figure 3). The TEM images of the heat-treated PVP- and PVA-Pt/Al$_2$O$_3$ catalysts show that no changes in the size of Pt NPs occurred after treatment. The high-resolution (HR)TEM images of Pt NPs clearly show lattice fringes with lattice spacings of 0.23 and 0.20 nm, corresponding to the {111} and {200} facets, respectively.[34,35] These polyhedral Pt NPs have similar mean diameters of 3 nm for all Pt catalysts.

The physical properties of PVP-, PVA-, and IMP-Pt/Al$_2$O$_3$ are listed in Table 1. Before heat treatment, only a small amount of CO was adsorbed on the Pt surface of the PVP- and PVA-Pt/Al$_2$O$_3$ catalysts because of the strongly preadsorbed capping agents. However, the amount of chemisorbed CO increased approximately 5−8 times after the heat treatment of the catalysts. This observation confirms that the capping agents on the Pt surface had been removed by the treatment at 623 K in an air atmosphere. The increase in the CO uptake was more noticeable for PVA-Pt/Al$_2$O$_3$ than for PVP-Pt/Al$_2$O$_3$. This

result is consistent with the weight loss of the Pt catalysts on removal of the capping agents, as shown in Figure 2, in which the lower thermal stability of PVA than that of PVP was revealed. The average sizes of the Pt NPs estimated by CO chemisorption, 7.2 nm for PVP-Pt/Al$_2$O$_3$ and 4.0 nm for PVA-Pt/Al$_2$O$_3$, are greater than those observed by TEM, 2.8−2.9 nm even after the removal of the capping agents. The overestimation is attributed to the presence of residual capping agents on the Pt surfaces, inhibiting CO chemisorption.

The presence of residual capping agents on the Pt surface was confirmed by comparing the FTIR spectra of PVP- and PVA-Pt/Al$_2$O$_3$ with those of intact capping agents. The support material, Al$_2$O$_3$, yielded absorption bands corresponding to the bending vibration of the hydroxyl group (3498 cm^{-1}) and H$_2$O bending vibrations (1632 cm^{-1}), as well as a broad peak corresponding to Al−O−Al bending (868 cm^{-1}) (Figure S1). The positions of these absorption bands of Al$_2$O$_3$ are consistent with previous reports.[36] The reference catalyst, IMP-Pt/Al$_2$O$_3$, showed absorption bands identical to those of the Al$_2$O$_3$ support. These results indicate that IMP-Pt/Al$_2$O$_3$ has clean Pt surfaces without any organic species.

The FTIR spectra of PVP- and PVA-Pt/Al$_2$O$_3$ obtained before and after heat treatment were compared with those of intact capping agents (Figure 4). Pure PVP yielded absorption bands corresponding to the pyrrolidone group (2956 and 2874 cm^{-1}), C=O stretching (1660 cm^{-1}), CH$_2$ bending (1461 cm^{-1}), CH bending (1425 cm^{-1}), and C−N bending (1280 cm^{-1}).[37−40] Before heat treatment, the spectrum of PVP-Pt/Al$_2$O$_3$ also contained the characteristic absorption bands of PVP, indicating that a significant amount of PVP remained adsorbed on the Pt surface. Compared to pure PVP, the PVP-Pt/Al$_2$O$_3$ catalyst exhibited a different feature at 1580 cm^{-1} in the spectrum. This seems to arise from the formation of strong C=O−Pt bonds.[37,38] A red shift of the PVP carbonyl frequency is attributed to the decrease in electron density in the C=O group by strong charge−transfer interactions with Pt NPs. After heat treatment, the bands in the spectrum were attenuated because of the removal of the adsorbed PVP from the Pt surface. As a result, the bands corresponding to the pyrrolidone group (2956 and 2874 cm^{-1}) were absent. However, the heat-treated PVP-Pt/Al$_2$O$_3$ showed a similar FTIR spectrum to that obtained before heat treatment, exhibiting absorption bands corresponding to CH$_2$ bending (1461 cm^{-1}) and CH bending (1425 cm^{-1}) modes. This indicates the presence of residual PVP on the Pt surface after heat treatment. The FTIR spectra of PVA-Pt/Al$_2$O$_3$ before and after heat treatment were also obtained. The characteristic absorption bands of PVA arising from CH$_2$ asymmetric stretching (2948 and 2897 cm^{-1}), CH stretching (2850 cm^{-1}), and C−OH stretching (1384 cm^{-1}) were observed for both catalysts.[40−43] These results indicate that despite heat treatment, residual PVP and PVA remained on the Pt surface. Moreover, the fact that both heat-treated PVP- and PVA-Pt/Al$_2$O$_3$ exhibited a lower CO uptake than IMP-Pt/Al$_2$O$_3$ (see Table 1) suggests that these residual capping agents could affect the adsorption behavior of reacting species during the reaction.

3.2. Distinct Effects of Residual Capping Agents in Enantioselective Hydrogenation. The catalytic performance of 1 wt % Pt/Al$_2$O$_3$ catalysts, the heat-treated PVP- and PVA-Pt/Al$_2$O$_3$, was investigated in the enantioselective hydrogenation of α-keto esters, EtPy and MtPy. IMP-Pt/Al$_2$O$_3$, which has a clean Pt surface, was used as a reference
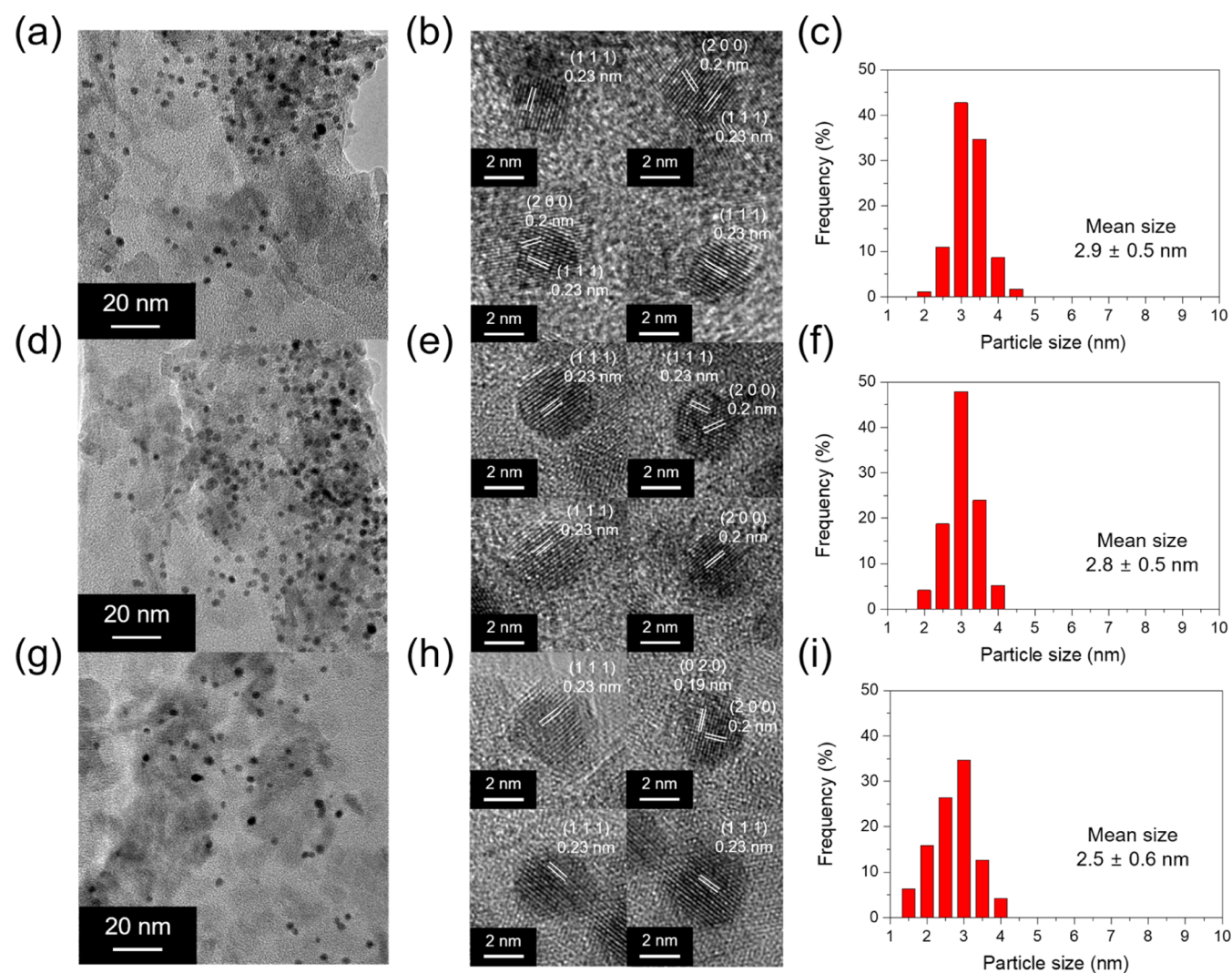
Figure 3. TEM images, HRTEM images, and size distribution histograms of Pt NPs for heat-treated (a–c) PVP-Pt/Al$_2$O$_3$, (d–f) PVA-Pt/Al$_2$O$_3$, and (g–i) IMP-Pt/Al$_2$O$_3$. The Pt NPs of all catalysts have similar average sizes and morphologies.

Table 1. Pt Loading, Total Amount of Adsorbed CO, Pt Dispersion, and Average Size of Pt NPs for PVP-Pt/Al$_2$O$_3$, PVA-Pt/Al$_2$O$_3$, and IMP-Pt/Al$_2$O$_3$

catalyst	Pt loading[a] [wt %]	before heat treatment		after heat treatment			
		CO uptake [μmol/g$_{cat}$]	D^b [%]	CO uptake [μmol/g$_{cat}$]	D^b [%]	$d_{CO}{}^c$ [nm]	$d_{TEM}{}^d$ [nm]
PVP-Pt/Al$_2$O$_3$	1.1	1.7	3.3	8.0	15.7	7.2	2.9
PVA-Pt/Al$_2$O$_3$	1.0	2.2	3.7	17.3	28.7	4.0	2.8
IMP-Pt/Al$_2$O$_3$	1.0			19.7	42.6	2.7	2.5

[a]Pt loading determined by ICP-OES. [b]Pt dispersion determined by CO chemisorption. [c]Average particle size of Pt NPs determined by CO chemisorption. [d]Average particle size of Pt NPs determined by TEM.

catalyst. The TOF and ee's of the Pt catalysts in the enantioselective hydrogenation of EtPy at 0.1 MPa H$_2$ pressure are listed in Table 2. In the absence of the chiral modifier, PVP- and PVA-Pt/Al$_2$O$_3$ showed lower TOF values than IMP-Pt/Al$_2$O$_3$. This is consistent with the CO chemisorption results listed in Table 1, which revealed lower CO uptake for both catalysts compared to that of IMP-Pt/Al$_2$O$_3$. Indeed, the lower TOF of PVP- and PVA-Pt/Al$_2$O$_3$ was attributed to the blockage of Pt sites for the adsorption of reacting species by residual capping agents.

Chiral modification of Pt catalysts by CD and QN not only led to enantioselectivity but also resulted in rate enhancement.

The significant rate acceleration caused by the presence of the cinchona alkaloids is an intrinsic phenomenon in enantioselective hydrogenation of α-keto esters over Pt catalysts.[5,9,11,44] The rate enhancement induced by the chiral modifier in the hydrogenation of EtPy decreased in the following order: PVP-Pt/Al$_2$O$_3$ > IMP-Pt/Al$_2$O$_3$ > PVA-Pt/Al$_2$O$_3$. Compared to use of the unmodified Pt catalyst, the use of the CD-modified IMP-Pt/Al$_2$O$_3$ catalyst led to a 1.9 times higher TOF, but that of the CD-modified PVP-Pt/Al$_2$O$_3$ catalyst led to a 2.5 times higher TOF. However, the TOF of the CD-modified PVA-Pt/Al$_2$O$_3$ catalyst was increased by only 1.4 times. A more noticeable rate enhancement effect in Pt catalysts was observed
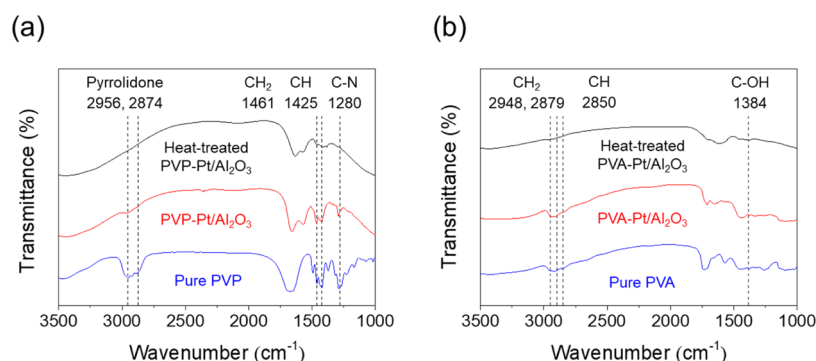
Figure 4. FTIR spectra of (a) intact PVP, PVP-Pt/Al$_2$O$_3$, and heat-treated PVP-Pt/Al$_2$O$_3$ and (b) intact PVA, PVA-Pt/Al$_2$O$_3$, and heat-treated PVA-Pt/Al$_2$O$_3$. The presence of the characteristic absorption bands of the capping agents indicates that residual PVP and PVA remain on the Pt surface after heat treatment.

Table 2. TOF [h^{-1}] and ee[a] [%] of Chirally Modified Pt/Al$_2$O$_3$ Catalysts in the Enantioselective Hydrogenation of EtPy[b] (Letters in Parentheses Represent the Chirality of the Major Product)

catalyst	modifier	TOF [h^{-1}]	ee [%]
PVP-Pt/Al$_2$O$_3$	none	190[c]	
	CD	480[c]	78 (R)
	QN	1480[c]	92 (R)
PVA-Pt/Al$_2$O$_3$	none	260[c]	
	CD	360[c]	33 (R)
	QN	460[c]	44 (R)
IMP-Pt/Al$_2$O$_3$	none	350[d]	
	CD	660[d]	46 (R)
	QN	990[d]	64 (R)

[a]ee [%] measured at 100% conversion. [b]Reaction conditions: 80 mg of the catalyst, 4 mg of the chiral modifier, 0.1 mL of EtPy, 10 mL of acetic acid, 0.1 MPa H$_2$ pressure, and 298 K. [c]TOF [h^{-1}] based on the number of surface Pt atoms predicted by a theoretical Pt NP model with an average particle size of 3 nm (Pt$_{923}$). [d]TOF [h^{-1}] based on the number of surface Pt atoms determined by CO chemisorption.

when QN was used. The QN-modified PVP-Pt/Al$_2$O$_3$ catalyst showed a TOF of 7.8 times higher than that of the unmodified catalyst, whereas QN-modified IMP- and PVA-Pt/Al$_2$O$_3$ exhibited only 2.8 and 1.8 times higher TOFs, respectively. In this case, the differences in the rate increase strongly depend on the presence and type of residual capping agents. Considering the critical role of cinchona alkaloids in rate acceleration, these results suggested that the residual species preadsorbed on the Pt surface significantly affect the adsorption behavior of the chiral modifiers.[45]

For chirally modified Pt catalysts, the ee values at full conversion are also listed in Table 2. The order of enantioselectivity of the chiral Pt/Al$_2$O$_3$ catalysts was identical to the order of rate acceleration: PVP-Pt/Al$_2$O$_3$ > IMP-Pt/Al$_2$O$_3$ > PVA-Pt/Al$_2$O$_3$. The positive correlation between enantioselectivity and activity is consistent with the results of previous reports.[11,46] The use of QN-modified Pt catalysts led to a higher ee than that of the CD-modified catalysts. In the case of IMP-Pt/Al$_2$O$_3$, CD- and QN-modified catalysts gave 46 and 64% ee, respectively. However, CD- and QN-modified PVP-Pt/Al$_2$O$_3$ exhibited remarkably higher enantioselectivities than the modified IMP-Pt/Al$_2$O$_3$, yielding 78 and 92% ee, respectively. It is noteworthy that the QN-modified PVP-Pt/Al$_2$O$_3$ with 1 wt % Pt loading showed comparable

enantioselectivity with those obtained from 5 wt % Pt/Al$_2$O$_3$, which is one of the most efficient catalysts, despite its lower loading.[47,48] More importantly, the presence of residual species of PVP on the Pt catalysts had a positive effect after chiral modification. To the best of our knowledge, this is the first demonstration of an enhancing effect of residual species of capping agents on both activity and selectivity in heterogeneous enantioselective catalysis. In contrast, CD- and QN-modified PVA-Pt/Al$_2$O$_3$ exhibited lower enantioselectivity than IMP-Pt/Al$_2$O$_3$, yielding 33 and 44% ee, respectively. These results indicate that the residual PVP on the Pt surface enhanced the performance for the enantioselective hydrogenation of EtPy, whereas the residual PVA worsened the catalytic properties.

The effect of residual capping agents on the catalytic performance was also investigated for the enantioselective hydrogenation of MtPy. The TOFs and ee's are summarized in Table 3. Similar trends in the catalytic performance to that of the enantioselective hydrogenation of EtPy were observed. Unmodified PVP- and PVA-Pt/Al$_2$O$_3$ exhibited lower TOFs than IMP-Pt/Al$_2$O$_3$ because the residual capping agents hindered the adsorption of reacting species on Pt sites. However, chirally modified PVP-Pt/Al$_2$O$_3$ showed a signifi-

Table 3. TOF [h^{-1}] and ee[a] [%] of Chirally Modified Pt/Al$_2$O$_3$ Catalysts in the Enantioselective Hydrogenation of MtPy[b] (Letters in Parentheses Represent the Chirality of the Major Product)

catalyst	modifier	TOF [h^{-1}]	ee [%]
PVP-Pt/Al$_2$O$_3$	none	90[c]	
	CD	820[c]	82 (R)
	QN	1810[c]	93 (R)
PVA-Pt/Al$_2$O$_3$	none	210[c]	
	CD	300[c]	38 (R)
	QN	630[c]	67 (R)
IMP-Pt/Al$_2$O$_3$	none	340[d]	
	CD	740[d]	54 (R)
	QN	1190[d]	72 (R)

[a]ee [%] measured at 100% conversion. [b]Reaction conditions: 80 mg of the catalyst, 4 mg of the chiral modifier, 0.1 mL of MtPy, 10 mL of acetic acid, 0.1 MPa H$_2$ pressure, and 298 K. [c]TOF [h^{-1}] based on the number of surface Pt atoms predicted using a theoretical Pt NP model with an average particle size of 3 nm (Pt$_{923}$). [d]TOF [h^{-1}] based on the number of surface Pt atoms determined by CO chemisorption.
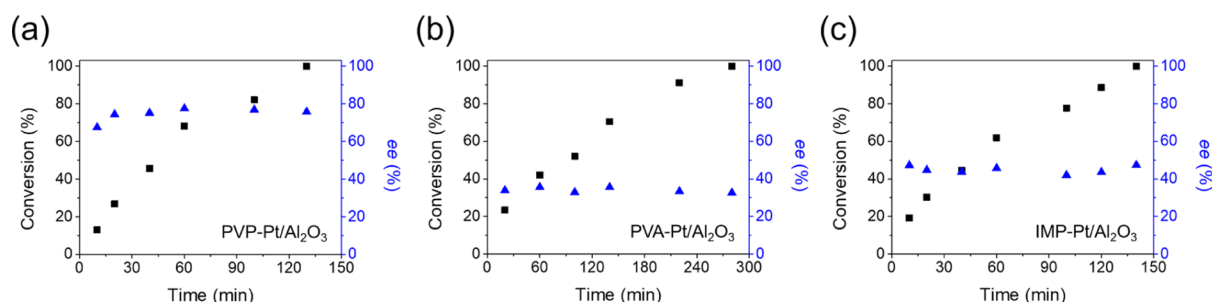
Figure 5. Plots of the conversion and ee of (a) PVP-Pt/Al$_2$O$_3$, (b) PVA-Pt/Al$_2$O$_3$, and (c) IMP-Pt/Al$_2$O$_3$ for the hydrogenation of EtPy[a] as a function of reaction time. No significant change in ee is observed during the reaction, indicating that residual capping agents, PVP and PVA, are stable on the Pt surface during the reaction. [a]Reaction conditions: 80 mg of the catalyst, 4 mg of CD, 0.1 mL of EtPy, 10 mL of acetic acid, 0.1 MPa H$_2$ pressure, and 298 K.

Table 4. Effect of H$_2$ Pressure on TOF [h^{-1}] and ee [%] of CD-Modified Pt/Al$_2$O$_3$ Catalysts in Enantioselective Hydrogenation of EtPy and MtPy[a]

	hydrogenation of EtPy				hydrogenation of MtPy			
	P_{H_2} = 0.1 MPa		P_{H_2} = 5.0 MPa		P_{H_2} = 0.1 MPa		P_{H_2} = 5.0 MPa	
catalyst	TOF [h^{-1}]	ee [%]	TOF [h^{-1}]	ee [%]	TOF [h^{-1}]	ee [%]	TOF [h^{-1}]	ee [%]
PVP-Pt/Al$_2$O$_3$	480[b]	78	2080[b]	91	820[b]	81	4500[b]	95
PVA-Pt/Al$_2$O$_3$	360[b]	33	1010[b]	57	300[b]	38	2630[b]	66
IMP-Pt/Al$_2$O$_3$	660[c]	46	1060[c]	55	740[c]	54	2130[c]	63

[a]Reaction conditions: 80 mg of the catalyst, 4 mg of CD, 0.1 mL of the substrate, 10 mL of acetic acid, 0.1 or 5.0 MPa H$_2$ pressure, and 298 K. [b]TOF [h^{-1}] based on the number of surface Pt atoms predicted using a theoretical Pt NP model with an average particle size of 3 nm (Pt$_{923}$). [c]TOF [h^{-1}] based on the number of surface Pt atoms determined by CO chemisorption.

cantly improved TOF compared to the modified IMP-Pt/Al$_2$O$_3$. In the case of PVA-Pt/Al$_2$O$_3$, chiral modification led to the lowest rate enhancement. The enantioselectivity of the chirally modified Pt catalysts showed a positive correlation with activity. The CD- and QN-modified IMP-Pt/Al$_2$O$_3$ exhibited 54 and 72% ee, respectively. The chiral PVP-Pt/Al$_2$O$_3$ led to a significant improvement in enantioselectivity, yielding 82% ee for CD and 93% ee for QN. However, chiral PVA-Pt/Al$_2$O$_3$ exhibited lower enantioselectivity than the corresponding IMP-Pt/Al$_2$O$_3$, showing only 38% ee for CD and 67% ee for QN. The order of activity and enantioselectivity of the chiral Pt/Al$_2$O$_3$ catalysts in the enantioselective hydrogenation of EtPy and MtPy was the same: PVP-Pt/Al$_2$O$_3$ > IMP-Pt/Al$_2$O$_3$ > PVA-Pt/Al$_2$O$_3$. These results clearly show that the enhancement and loss of the catalytic performance can be attributed to the residual capping agents.

During enantioselective hydrogenation, the residual capping agents could be desorbed from the Pt surface. Indeed, a Pt/SiO$_2$ catalyst capped by PAA and PAA-Pt/SiO$_2$ yields a poor ee during the initial reaction period at 0.1 MPa H$_2$ pressure.[11] However, a rapid enhancement in enantioselectivity is observed once the PAA capping agents have been removed from the Pt surface under reaction conditions. In our case, the removal of residual PVP and PVA would lead to a decrease and increase in the catalytic performance, respectively. The stability of residual capping agents on the Pt surface was investigated by monitoring the change in the performance of the PVP-, PVA-, and IMP-Pt/Al$_2$O$_3$ catalysts as a function of reaction time during the enantioselective hydrogenation of EtPy (Figure 5). For both CD-modified PVP- and PVA-Pt/Al$_2$O$_3$ catalysts, enantioselectivity was determined in the early stages of the reaction. Subsequently, there was no significant change. A comparison with the case of IMP-Pt/Al$_2$O$_3$ showed that the

residual PVP and PVA capping agents were stable on the Pt surface during the reaction at 0.1 MPa H$_2$ pressure.

Additionally, the influence of H$_2$ pressure on the catalytic performance of the Pt catalysts with residual capping agents was investigated because CD-modified Pt catalysts, in general, exhibit enhanced enantioselectivity at high H$_2$ pressures.[22,49,50] The TOFs and ee's of the CD-modified Pt catalysts in the enantioselective hydrogenation of α-keto esters at 0.1 and 5.0 MPa H$_2$ pressure are compared in Table 4. Similar to the reference catalyst, IMP-Pt/Al$_2$O$_3$, both PVP- and PVA-Pt/Al$_2$O$_3$ catalysts showed improved activity and enantioselectivity. Among the Pt catalysts, PVP-Pt/Al$_2$O$_3$ exhibited the highest enantioselectivity at 5.0 MPa H$_2$ pressure, yielding 91% ee in the hydrogenation of EtPy and 95% ee in the hydrogenation of MtPy, respectively. The increase in the enantioselectivity of PVP-Pt/Al$_2$O$_3$ at high H$_2$ pressure was greater than that of IMP-Pt/Al$_2$O$_3$. This indicates that the residual PVP, which had a positive effect for enantioselective hydrogenation, was stable on the Pt surface, even at 5.0 MPa H$_2$ pressure. In the case of PVA-Pt/Al$_2$O$_3$, the lowest TOF and ee value were observed at 0.1 MPa H$_2$ pressure. At 5.0 MPa H$_2$ pressure, however, it exhibited performance similar to that of IMP-Pt/Al$_2$O$_3$, showing that the detrimental effect of the residual PVA was negligible at high H$_2$ pressure. It is also noteworthy that there have been attempts to use PVP-stabilized Pt NPs for heterogeneous enantioselective hydrogenation in which the PVP on Pt NPs of Pt/Al$_2$O$_3$ was rinsed out before the reaction.[51,52] The washed Pt/Al$_2$O$_3$ exhibited approximately 84% ee in hydrogenation of MtPy at high H$_2$ pressure.[52] This suggests that the method for post-treatment of polymer-capped Pt NPs could significantly affect the catalytic performance in enantioselective hydrogenation.

Although the nearly constant enantioselectivity during the reaction at 0.1 MPa H$_2$ pressure (see Figure 5) confirms the

stability of PVA on the Pt surface, we could not rule out the possibility that the removal of PVA contributed to the improvement in enantioselectivity at 5.0 MPa H_2 pressure. Thus, the ee values for enantioselective hydrogenation of EtPy were measured again at 0.1 MPa H_2 pressure after the treatment of the Pt catalysts at 5.0 MPa H_2 pressure for 2 h (Table 5). There were no significant changes in the TOF and

Table 5. Effect of H_2 Treatment[a] of CD-Modified Pt/Al$_2$O$_3$ Catalysts on TOF $[h^{-1}]$ and ee [%] in the Enantioselective Hydrogenation of EtPy[b]

catalyst	before H_2 treatment		after 2 h H_2 treatment	
	TOF $[h^{-1}]$	ee [%]	TOF $[h^{-1}]$	ee [%]
PVP-Pt/Al$_2$O$_3$	480	78	420	77
PVA-Pt/Al$_2$O$_3$	360	33	710	51
IMP-Pt/Al$_2$O$_3$	660	46	550	45

[a]H_2 treatment conditions: 80 mg of the catalyst, 4 mg of the chiral modifier, 10 mL of acetic acid, 5.0 MPa H_2 pressure, and 298 K. [b]Reaction conditions: 80 mg of the catalyst, 4 mg of the chiral modifier, 0.1 mL of EtPy, 10 mL of acetic acid, 0.1 MPa H_2 pressure, and 298 K.

ee of IMP-Pt/Al$_2$O$_3$. As expected, the treated PVP-Pt/Al$_2$O$_3$ yielded a nearly identical performance to that before H_2 treatment, showing that the residual PVP was stable on the Pt surface after H_2 treatment at high pressure. However, H_2 treatment of PVA-Pt/Al$_2$O$_3$ at 5.0 MPa led to an increase in activity and enantioselectivity from 33 to 51% ee. A similar change was observed for the treated Pt catalysts in enantioselective hydrogenation of MtPy (Table S1). These results are consistent with the removal of the residual PVA and, thus, the attenuation of the detrimental effect of PVA on the catalytic performance under high H_2 pressure conditions.

3.3. Selective Exposure of Pt Sites by Residual Capping Agents. To elucidate the origin of the significant change in the catalytic performance of PVP- and PVA-Pt/Al$_2$O$_3$ for enantioselective hydrogenation, the electronic states of the Pt catalysts were investigated by XPS. The Pt 4d XPS spectra of PVP-, PVA-, and IMP-Pt/Al$_2$O$_3$ are compared in Figure 6. The spectrum of the reference catalyst, IMP-Pt/Al$_2$O$_3$, contains Pt 4d$_{3/2}$ and Pt 4d$_{5/2}$ peaks at binding energies of 315.0 and 332.0 eV, respectively. These binding energies confirm that IMP-Pt/Al$_2$O$_3$ had a clean Pt surface without
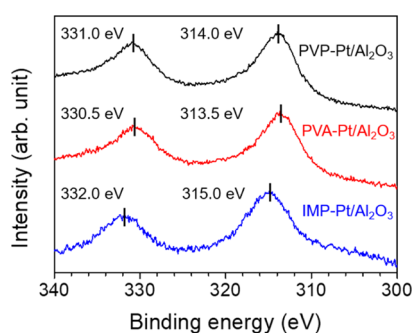
Figure 6. X-ray photoelectron spectra of the Pt 4d region for heat-treated Pt catalysts. The lower binding energies of the peaks for PVP-Pt/Al$_2$O$_3$ and PVA-Pt/Al$_2$O$_3$ compared to those of IMP-Pt/Al$_2$O$_3$ indicate the presence of residual capping agents on the Pt surface and increased electron density of Pt induced by the presence of surface species.

residual capping agents and was in the metallic state.[53−55] For both PVP- and PVA-Pt/Al$_2$O$_3$, however, there was a peak shift to lower binding energies by about 1.0−1.5 eV. This is consistent with previous reports concerning the change in the electron density of Pt by the residual PVP and PVA species.[56,57] The XPS results show the presence of residual capping agents on the Pt surface and an increase in the electron density of Pt by electron transfer from the organic species. Nonetheless, the fact that PVP- and PVA-Pt/Al$_2$O$_3$ showed opposing catalytic performance indicates that the increase in the electron density of Pt was not an important factor determining their enantioselectivity.

Enantioselective hydrogenation of α-keto esters is structure sensitive, and the enantioselectivity strongly depends on the exposed sites on the Pt NPs.[9,11,12,29] Thus, the exposed Pt sites of PVP-, PVA-, and IMP-Pt/Al$_2$O$_3$ were examined by DRIFTS measurements of CO-adsorbed samples. The vibrational frequencies of CO molecules linearly adsorbed on Pt catalysts are site-specific and, thus, provide information about the type of exposed Pt sites, such as well-coordinated (WC; terrace) sites and under-coordinated (UC; step, edge, and corner) sites.[58] The DRIFT spectra of adsorbed CO on the Pt catalysts are compared in Figure 7. The spectrum of IMP-Pt/Al$_2$O$_3$
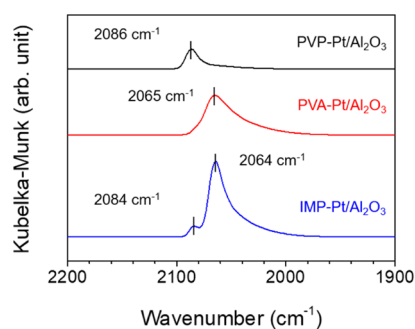
Figure 7. DRIFT spectra of CO adsorbed on PVP-Pt/Al$_2$O$_3$, PVA-Pt/Al$_2$O$_3$, and IMP-Pt/Al$_2$O$_3$. The peaks at 2084 and 2064 cm^{-1} can be assigned to linearly adsorbed CO on WC and UC Pt sites, respectively. Compared to the spectrum of IMP-Pt/Al$_2$O$_3$, those of PVP- and PVA-Pt/Al$_2$O$_3$ contain only one peak, indicating the selective exposure of WC Pt sites for PVP-Pt/Al$_2$O$_3$ and UC Pt sites for PVA-Pt/Al$_2$O$_3$.

contains two peaks at 2084 and 2064 cm^{-1}. These were assigned to the vibrational stretches of CO molecules linearly adsorbed on WC and UC, respectively.[58] The noticeable difference in peak intensity is attributed to the fact that the extinction coefficient for the stretch arising from CO adsorbed on UC Pt sites is 2.7 times greater than that arising from CO adsorbed on WC Pt sites.[59] The spectrum of IMP-Pt/Al$_2$O$_3$ confirms that it contains both WC and UC Pt sites for the adsorption of reacting species during enantioselective hydrogenation. However, the spectrum of PVP-Pt/Al$_2$O$_3$ exhibited only one peak at 2086 cm^{-1}, indicating adsorption of CO molecules on WC Pt sites. The exclusive exposure of WC sites on the Pt surface showed that PVP on WC Pt sites was effectively removed during heat treatment, whereas PVP on UC Pt sites was not. In contrast, the spectrum of PVA-Pt/Al$_2$O$_3$ exhibited only one peak at 2065 cm^{-1}, indicating adsorption of CO molecules on the UC Pt sites. This suggests that residual PVA remained on the WC Pt sites, exposing only the UC sites after heat treatment. It has been reported that intact PVP and PVA show preferential adsorption on the
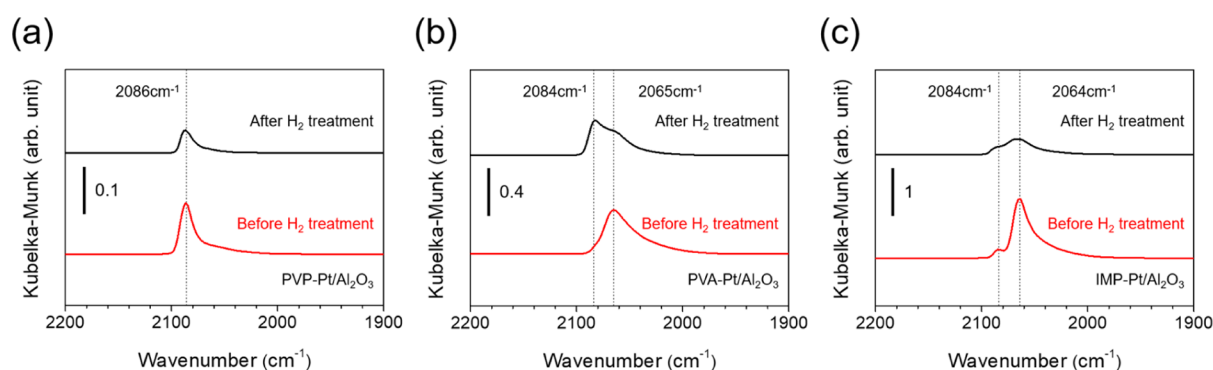
Figure 8. DRIFT spectra of CO adsorbed on (a) PVP-Pt/Al$_2$O$_3$, (b) PVA-Pt/Al$_2$O$_3$, and (c) IMP-Pt/Al$_2$O$_3$ before and after H$_2$ treatment at 5.0 MPa H$_2$ pressure. There are no changes in the type of exposed Pt sites for IMP-Pt/Al$_2$O$_3$ and PVP-Pt/Al$_2$O$_3$. In contrast, the appearance of a peak at 2084 cm^{-1}, arising from adsorbed CO on Pt terrace sites, indicates the removal of the residual PVA under high H$_2$ pressure and the additional exposure of the WC Pt sites of PVA-Pt/Al$_2$O$_3$.

defect sites of the Pt surface and {111} facets of the Pd surface, respectively.[60−62] Our case is interesting in that heat treatment of polymer-capped Pt NPs can lead to the exclusive blockage of defect or terrace sites by residual capping agents. These results seem to be related to differences in thermal stability rather than the adsorption energies of the capping agents on surface sites having different coordination structures.

Compared to IMP-Pt/Al$_2$O$_3$, PVP-Pt/Al$_2$O$_3$ exhibited superior catalytic performance and PVA-Pt/Al$_2$O$_3$ exhibited inferior performance in the enantioselective hydrogenation of EtPy and MtPy. The DRIFT spectra of CO adsorbed on Pt catalysts showed that the residual capping agents directly affected the catalytic performance by selectively exposing Pt sites. In enantioselective hydrogenation over cinchona alkaloid-modified Pt catalysts, large and flat ensembles of Pt atoms are required to accommodate the bulky CD and QN chiral modifiers and their complex interacting with the reactant.[29] Moreover, cinchona alkaloids are stabilized on terrace sites via π−π interactions between the quinoline ring and the Pt surface.[13] Therefore, the higher performance of PVP-Pt/Al$_2$O$_3$ having exposed terraces than that of PVA-Pt/Al$_2$O$_3$ having exposed defects was attributed to the stable adsorption of the chiral modifiers and the efficient creation of chiral Pt sites. Our results are consistent with previous observations that larger Pt NPs with more terrace sites than defect sites show higher performance.

Although PVA-Pt/Al$_2$O$_3$ showed inferior enantioselectivity at 0.1 MPa H$_2$ pressure, it exhibited nearly the same ee values as IMP-Pt/Al$_2$O$_3$ at 5.0 MPa H$_2$ pressure. As shown by the data in Table 5, the improvement in enantioselectivity is most likely due to the removal of residual PVA from the Pt surface at high H$_2$ pressures. The DRIFT spectra of CO adsorbed on PVP-, PVA-, and IMP-Pt/Al$_2$O$_3$ were obtained after H$_2$ treatment at 5.0 MPa to confirm the changes in the exposed Pt sites (Figure 8). Although there is a change in the intensity ratio of the peaks, which seems to arise from residual solvent molecules on the treated catalyst, the spectrum of IMP-Pt/Al$_2$O$_3$ still contains peaks at 2084 and 2064 cm^{-1} after treatment, confirming the presence of WC and UC Pt sites, respectively. There is no change in the type of the exposed Pt sites for PVP-Pt/Al$_2$O$_3$, as shown by its spectrum, which only contains a peak at 2086 cm^{-1}. The appearance of a single peak arising from the stretch of CO adsorbed on WC Pt sites again indicates that the residual PVP covering the UC Pt sites was stable even after H$_2$ treatment at high pressure. The

observation that there was no change in the type of exposed Pt sites clearly supports the constant enantioselectivity of IMP- and PVP-Pt/Al$_2$O$_3$ before and after H$_2$ treatment. In the case of the spectrum of PVA-Pt/Al$_2$O$_3$, the peak at 2065 cm^{-1} is still present. However, a new peak, which was not observed before H$_2$ treatment, appears at 2084 cm^{-1}. Thus, it was concluded that the removal of the residual PVA by H$_2$ treatment and subsequent exposure of WC Pt sites, that is, terraces, led to an increase in the enantioselectivity of PVA-Pt/Al$_2$O$_3$. The DRIFT results demonstrate that site-selective exposure of the Pt surface by residual capping agents is a key factor determining the catalytic performance. In addition, these results show that terrace sites are more efficient than defect sites in the enantioselective hydrogenation of α-keto esters.

As mentioned above, stable adsorption of a chiral modifier on the Pt surface is an important prerequisite for achieving high enantioselectivity. Thus, the amount of CD adsorbed on the Pt surface was estimated by comparing the CO uptake before and after CD adsorption in which the CO uptake of a Pt catalyst is proportional to the number of exposed Pt sites on the surface. The CO uptake values for IMP-, PVP-, and PVA-Pt/Al$_2$O$_3$ are summarized in Table 6. Both PVP- and PVA-Pt/

Table 6. Change in the Amount of CO Uptake Before and After the Adsorption of CD Modifier on Pt/Al$_2$O$_3$ Catalysts

catalyst	before CD adsorption CO uptake (B) [μmol/g$_{cat}$]	after CD adsorption CO uptake (A) [μmol/g$_{cat}$]	absolute decrease in CO uptake [μmol/g$_{cat}$]	relative decrease in CO uptake[a] [%]
PVP-Pt/Al$_2$O$_3$	8.0	1.5	6.5	81.3
PVA-Pt/Al$_2$O$_3$	17.3	14.8	2.5	14.5
IMP-Pt/Al$_2$O$_3$	19.7	12.2	7.5	38.1

$^a(B − A)/B \times 100$ [%].

Al$_2$O$_3$ exhibited less CO uptake than IMP-Pt/Al$_2$O$_3$ because of the blockage of Pt sites by residual capping agents. After the adsorption of CD, the strongly adsorbed chiral modifier on the Pt surface reduced the number of exposed Pt sites for the adsorption of CO. As a result, the CO uptake decreased noticeably for all Pt catalysts. Similar changes were observed in the CO chemisorption results of the Pt catalysts after the adsorption of QN (Table S2).
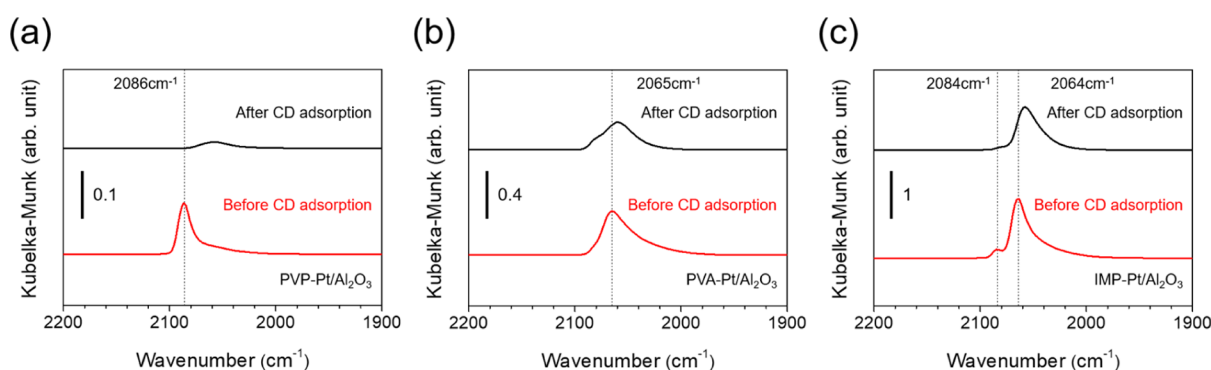
Figure 9. DRIFT spectra of CO adsorbed on (a) PVP-Pt/Al$_2$O$_3$, (b) PVA-Pt/Al$_2$O$_3$, and (c) IMP-Pt/Al$_2$O$_3$ before and after CD adsorption. The peak at approximately 2085 cm^{-1} arising from the CO adsorbed on WC Pt sites disappears after CD adsorption. This indicates preferential and stable adsorption of CD on Pt terrace sites rather than Pt defect sites.

The DRIFT spectra of adsorbed CO in Figure 7 indicate that PVP-Pt/Al$_2$O$_3$ only exposes WC Pt sites, whereas IMP-Pt/Al$_2$O$_3$ exposes both WC and UC Pt sites. Therefore, CD could adsorb on the exposed WC Pt sites for PVP-Pt/Al$_2$O$_3$ and on both WC and UC sites for IMP-Pt/Al$_2$O$_3$. Interestingly, the absolute decrease in the CO uptake for PVP-Pt/Al$_2$O$_3$ was similar to that for IMP-Pt/Al$_2$O$_3$ despite the fact that PVP-Pt/Al$_2$O$_3$ initially has less than half of the exposed Pt sites of IMP-Pt/Al$_2$O$_3$. However, the absolute decrease in the number of exposed sites in PVA-Pt/Al$_2$O$_3$ was noticeably smaller than those of other Pt catalysts. This result reveals that the selectively exposed defect sites of PVA-Pt/Al$_2$O$_3$ are inefficient adsorption sites for CD molecules. A comparison of the relative decrease in the CO uptake between Pt catalysts clearly shows that terrace sites are more suitable for the stable adsorption of CD than other defect sites such as steps, edges, and corners. Furthermore, PVP-Pt/Al$_2$O$_3$ showed higher enantioselectivity than IMP-Pt/Al$_2$O$_3$ despite the lower absolute decrease in the CO uptake. The fact that in the case of PVP-Pt/Al$_2$O$_3$, the chiral modifier was selectively adsorbed on terraces suggests that CD molecules on terrace sites are more efficient for enantiodifferentiation than those on defect sites.

The efficient adsorption of CD molecules on Pt terrace sites for the creation of chiral sites was also investigated by comparing the DRIFTS spectra of CO adsorbed on the Pt catalysts after the adsorption of CD (Figure 9). The spectrum of surface-clean IMP-Pt/Al$_2$O$_3$ contains two peaks corresponding to linearly adsorbed CO on the WC and UC Pt sites. After the adsorption of CD, the peak at 2064 cm^{-1} remains, whereas the peak at 2084 cm^{-1} disappears. This change confirms the strong and selective adsorption of CD molecules on WC Pt sites rather than on UC sites. Similarly, the peak arising from CO on the WC Pt sites of PVP-Pt/Al$_2$O$_3$ completely disappears after CD adsorption. On the other hand, there is no noticeable change in the CO-DRIFT spectra of PVA-Pt/Al$_2$O$_3$. The clear appearance of a peak at 2065 cm^{-1} after CD adsorption indicates unstable and weak adsorption of CD molecules on the UC sites, as shown for the case of IMP-Pt/Al$_2$O$_3$. Moreover, similar changes were observed in the CO-DRIFT spectra of the Pt catalysts after the adsorption of QN (Figure S2). These observations again confirm that the significant improvement in the catalytic performance of PVP-Pt/Al$_2$O$_3$ in the enantioselective hydrogenation of α-keto esters originated from the site-selective exposure of WC Pt

sites and the stable adsorption of the chiral modifier on the terrace sites.

4. CONCLUSIONS

Polymer-capped Pt/Al$_2$O$_3$ containing uniform sized Pt NPs was used as a heterogeneous catalyst for the enantioselective hydrogenation of α-keto esters. After the heat treatment of the Pt catalysts, the residual capping agents led to the site-selective blockage of Pt sites. As a result, the heat-treated PVP-Pt/Al$_2$O$_3$ exclusively exposed WC terrace sites, whereas the treated PVA-Pt/Al$_2$O$_3$ selectively exposed UC defect sites. The site-specific exposure of Pt sites significantly affected both the reaction rate and enantioselectivity. Compared to IMP-Pt/Al$_2$O$_3$ exposing both terraces and defects, PVP-Pt/Al$_2$O$_3$ showed remarkably enhanced catalytic performance, whereas PVA-Pt/Al$_2$O$_3$ exhibited inferior performance. The improvement in the catalytic performance of PVP-Pt/Al$_2$O$_3$ was attributed to the stable adsorption of a chiral modifier on terrace sites and their effective enantiodifferentiation. Our study provides a new strategy to develop site selectively exposed metal NPs and demonstrates the enhancing effect of residual capping agents on the catalytic properties in structure-sensitive reactions.

■ ASSOCIATED CONTENT

ⓈI Supporting Information

The Supporting Information is available free of charge at https://pubs.acs.org/doi/10.1021/acscatal.0c04255.

Performance for enantioselective hydrogenation of MtPy after H$_2$ treatment, FTIR spectra of Al$_2$O$_3$ and IMP-Pt/Al$_2$O$_3$, CO chemisorption results, and CO-DRIFT spectra of Pt catalysts after QN adsorption (PDF)

■ AUTHOR INFORMATION

Corresponding Author

Yongju Yun − *Department of Chemical Engineering, Pohang University of Science and Technology (POSTECH), Pohang, Gyeongbuk 37673, Republic of Korea;* ⓞ orcid.org/0000-0001-6497-4128; Email: yjyun@postech.ac.kr

Authors

Iljun Chung − *Department of Chemical Engineering, Pohang University of Science and Technology (POSTECH), Pohang, Gyeongbuk 37673, Republic of Korea*

Byeongju Song − *Department of Chemical Engineering, Pohang University of Science and Technology (POSTECH), Pohang, Gyeongbuk 37673, Republic of Korea*

Jeongmyeong Kim − *Department of Chemical Engineering, Pohang University of Science and Technology (POSTECH), Pohang, Gyeongbuk 37673, Republic of Korea*

Complete contact information is available at:
https://pubs.acs.org/10.1021/acscatal.0c04255

Author Contributions

†I.C. and B.S. equally contributed to this work.

Notes

The authors declare no competing financial interest.

■ REFERENCES

(1) Klingler, F. D. Asymmetric hydrogenation of prochiral amino ketones to amino alcohols for pharmaceutical use. *Acc. Chem. Res.* **2007**, *40*, 1367−1376.

(2) Kasprzyk-Hordern, B. Pharmacologically active compounds in the environment and their chirality. *Chem. Soc. Rev.* **2010**, *39*, 4466−4503.

(3) Sholl, D. S.; Gellman, A. J. Developing chiral surfaces for enantioselective chemical processing. *AIChE J.* **2009**, *55*, 2484−2490.

(4) Smith, S. W. Chiral Toxicology: It's the Same Thing...Only Different. *Toxicol. Sci.* **2009**, *110*, 4−30.

(5) Blaser, H.-U.; Jalett, H.-P.; Müller, M.; Studer, M. Enantioselective hydrogenation of α-ketoesters using cinchona modified platinum catalysts and related systems: A review. *Catal. Today* **1997**, *37*, 441−463.

(6) Meemken, F.; Baiker, A. Recent Progress in Heterogeneous Asymmetric Hydrogenation of C=O and C=C Bonds on Supported Noble Metal Catalysts. *Chem. Rev.* **2017**, *117*, 11522−11569.

(7) Heitbaum, M.; Glorius, F.; Escher, I. Asymmetric heterogeneous catalysis. *Angew. Chem., Int. Ed.* **2006**, *45*, 4732−4762.

(8) Orito, Y.; Imai, S.; Niwa, S.; Hung, N.-G. Asymmetric hydrogenation of methyl benzoylformate using platinum-carbon catalysts modified with cinchonidine. *J. Synth. Org. Chem., Jpn.* **1979**, *37*, 173−174.

(9) Mallat, T.; Orglmeister, E.; Baiker, A. Asymmetric catalysis at chiral metal surfaces. *Chem. Rev.* **2007**, *107*, 4863−4890.

(10) Meemken, F.; Hungerbühler, K.; Baiker, A. Monitoring surface processes during heterogeneous asymmetric hydrogenation of ketones on a chirally modified platinum catalyst by operando spectroscopy. *Angew. Chem., Int. Ed.* **2014**, *53*, 8640−8644.

(11) Schmidt, E.; Vargas, A.; Mallat, T.; Baiker, A. Shape-selective enantioselective hydrogenation on Pt nanoparticles. *J. Am. Chem. Soc.* **2009**, *131*, 12358−12367.

(12) Attard, G. A.; Griffin, K. G.; Jenkins, D. J.; Johnston, P.; Wells, P. B. Enantioselective hydrogenation of ethyl pyruvate catalysed by Pt/graphite: Superior performance of sintered metal particles. *Catal. Today* **2006**, *114*, 346−352.

(13) Kubota, J.; Zaera, F. Adsorption geometry of modifiers as key in imparting chirality to platinum catalysts. *J. Am. Chem. Soc.* **2001**, *123*, 11115−11116.

(14) Wehrli, J. T.; Baiker, A.; Monti, D. M.; Blaser, H. U. Enantioselective hydrogenation of α-ketoesters: Preparation and catalytic behavior of different alumina-supported platinum catalysts modified with cinchonidine. *J. Mol. Catal.* **1990**, *61*, 207−226.

(15) Azmat, M. U.; Guo, Y.; Guo, Y.; Wang, Y.; Lu, G. An easy and effective approach towards heterogeneous Pt/SiO$_2$-cinchonidine catalyst system for enantioselective hydrogenation of ethyl pyruvate. *J. Mol. Catal. A: Chem.* **2011**, *336*, 42−50.

(16) Chen, C.; Zhan, E.; Ta, N.; Li, Y.; Shen, W. Enantioselective hydrogenation of α,β-unsaturated carboxylic acids on Pd nanocubes. *Catal. Sci. Technol.* **2013**, *3*, 2620−2626.

(17) Su, N.; Gao, X.; Chen, X.; Yue, B.; He, H. The enantioselective hydrogenation of acetophenone over Pd concave tetrahedron nanocrystals affected by the residual adsorbed capping agent polyvinylpyrrolidone (PVP). *J. Catal.* **2018**, *367*, 244−251.

(18) Niu, Z.; Li, Y. Removal and utilization of capping agents in nanocatalysis. *Chem. Mater.* **2014**, *26*, 72−83.

(19) Schmidt, E.; Kleist, W.; Krumeich, F.; Mallat, T.; Baiker, A. Platinum nanoparticles: The crucial role of crystal face and colloid stabilizer in the diastereoselective hydrogenation of cinchonidine. *Chem. - Eur. J.* **2010**, *16*, 2181−2192.

(20) Han, Z.; Li, S.; Jiang, F.; Wang, T.; Ma, X.; Gong, J. Propane dehydrogenation over Pt-Cu bimetallic catalysts: the nature of coke deposition and the role of copper. *Nanoscale* **2014**, *6*, 10000−10008.

(21) Karelovic, A.; Ruiz, P. The role of copper particle size in low pressure methanol synthesis via CO$_2$ hydrogenation over Cu/ZnO catalysts. *Catal. Sci. Technol.* **2015**, *5*, 869−881.

(22) Kim, J.; Song, B.; Hwang, G.; Bang, Y.; Yun, Y. Platinum nanoparticles supported on mesocellular silica foams as highly efficient catalysts for enantioselective hydrogenation. *J. Catal.* **2019**, *373*, 306−313.

(23) Song, B.; Kim, J.; Chung, I.; Yun, Y., Mesoporous silica-supported Pt catalysts in enantioselective hydrogenation of ethyl pyruvate. *Catal. Today* **2020**, in press.

(24) Marinkovic, N. S.; Sasaki, K.; Adzic, R. R. Determination of single- and multi-component nanoparticle sizes by X-ray absorption spectroscopy. *J. Electrochem. Soc.* **2018**, *165*, J3222−J3230.

(25) Ustarroz, J.; Ornelas, I. M.; Zhang, G.; Perry, D.; Kang, M.; Bentley, C. L.; Walker, M.; Unwin, P. R. Mobility and poisoning of mass-selected platinum nanoclusters during the oxygen reduction reaction. *ACS Catal.* **2018**, *8*, 6775−6790.

(26) Li, L.; Abild-Pedersen, F.; Greeley, J.; Nørskov, J. K. Surface tension effects on the reactivity of metal nanoparticles. *J. Phys. Chem. Lett.* **2015**, *6*, 3797−3801.

(27) Li, L.; Larsen, A. H.; Romero, N. A.; Morozov, V. A.; Glinsvad, C.; Abild-Pedersen, F.; Greeley, J.; Jacobsen, K. W.; Nørskov, J. K. Investigation of catalytic finite-size-effects of platinum metal clusters. *J. Phys. Chem. Lett.* **2013**, *4*, 222−226.

(28) Ferri, D.; Bürgi, T. An in Situ Attenuated Total Reflection Infrared Study of a Chiral Catalytic Solid−Liquid Interface: Cinchonidine Adsorption on Pt. *J. Am. Chem. Soc.* **2001**, *123*, 12074−12084.

(29) Ni, Y.; Wang, Z.; Lee, I.; Zaera, F. Adsorption of chiral modifiers from solution onto supported platinum catalysts: The effect of the solvent, other coadsorbates, and the support. *J. Phys. Chem. C* **2020**, *124*, 7903−7913.

(30) Ziaei-Azad, H.; Semagina, N. Bimetallic catalysts: Requirements for stabilizing PVP removal depend on the surface composition. *Appl. Catal., A* **2014**, *482*, 327−335.

(31) Fiorio, J. L.; Barbosa, E. C. M.; Kikuchi, D. K.; Camargo, P. H. C.; Rudolph, M.; Hashmi, A. S. K.; Rossi, L. M. Piperazine-promoted gold-catalyzed hydrogenation: The influence of capping ligands. *Catal. Sci. Technol.* **2020**, *10*, 1996−2003.

(32) Rao, V.; Latha, P.; Ashokan, P. V.; Shridhar, M. H. Thermal degradation of poly(N-vinylpyrrolidone)-poly(vinyl alcohol) blends. *Polym. J.* **1999**, *31*, 887−889.

(33) Helberg, R. M. L.; Dai, Z. D.; Ansaloni, L.; Deng, L. Y. PVA/PVP blend polymer matrix for hosting carriers in facilitated transport membranes: Synergistic enhancement of CO$_2$ separation performance. *Green Energy Environ.* **2020**, *5*, 59−68.

(34) Miyazawa, K.; Yoshitake, M.; Tanaka, Y. HRTEM analyses of the platinum nanoparticles prepared on graphite particles using coaxial arc plasma deposition. *J. Nanopart. Res.* **2017**, *19*, 191.

(35) Wang, Z.; Suo, Q.; Zhang, C.; Chai, Z.; Wang, X. Solvent-controlled platinum nanocrystals with a high growth rate along < 100 > to < 111 > and enhanced electro-activity in the methanol oxidation reaction. *RSC Adv.* **2016**, *6*, 89098−89102.

(36) Gangwar, J.; Gupta, B. K.; Tripathi, S. K.; Srivastava, A. K. Phase dependent thermal and spectroscopic responses of Al$_2$O$_3$ nanostructures with different morphogenesis. *Nanoscale* **2015**, *7*, 13313−13344.

(37) Safo, I. A.; Dosche, C.; Özaslan, M. Effects of capping agents on the oxygen reduction reaction activity and shape stability of Pt nanocubes. *ChemPhysChem* **2019**, *20*, 3010−3023.

(38) Borodko, Y.; Habas, S. E.; Koebel, M.; Yang, P.; Frei, H.; Somorjai, G. A. Probing the interaction of poly (vinylpyrrolidone) with platinum nanocrystals by UV-Raman and FTIR. *J. Phys. Chem. B* **2006**, *110*, 23052−23059.

(39) Safo, I. A.; Werheid, M.; Dosche, C.; Oezaslan, M. The role of polyvinylpyrrolidone (PVP) as a capping and structure-directing agent in the formation of Pt nanocubes. *Nanoscale Adv.* **2019**, *1*, 3095−3106.

(40) Ajitha, B.; Kumar Reddy, Y. A.; Reddy, P. S.; Jeon, H.-J.; Ahn, C. W. Role of capping agents in controlling silver nanoparticles size, antibacterial activity and potential application as optical hydrogen peroxide sensor. *RSC Adv.* **2016**, *6*, 36171−36179.

(41) Hazarika, S. J.; Mohanta, D. Revealing mechanical, tribological, and surface-wettability features of nanoscale inorganic fullerene-type tungsten disulfide dispersed in a polymer. *J. Mater. Res.* **2019**, *34*, 3666−3677.

(42) Mansur, H. S.; Sadahira, C. M.; Souza, A. N.; Mansur, A. A. P. FTIR spectroscopy characterization of poly (vinyl alcohol) hydrogel with different hydrolysis degree and chemically crosslinked with glutaraldehyde. *Mater. Sci. Eng., C* **2008**, *28*, 539−548.

(43) Jia, B.; Zhao, Y.; Qin, M.; Zhang, Z.; Liu, L.; Wu, H.; Liu, Y.; Qu, X. A self-standing silver/crosslinked-poly(vinyl alcohol) network with microfibers, nanowires and nanoparticles and its linear aggregation. *J. Colloid Interface Sci.* **2019**, *535*, 524−532.

(44) Bürgi, T.; Baiker, A. Heterogeneous enantioselective hydrogenation over cinchona alkaloid modified platinum: Mechanistic insights into a complex reaction. *Acc. Chem. Res.* **2004**, *37*, 909−917.

(45) Tálas, E.; Margitfalvi, J. L.; Egyed, O. Additional data to the origin of rate enhancement in the enantioselective hydrogenation of activated ketones over cinchonidine modified platinum catalyst. *J. Catal.* **2009**, *266*, 191−198.

(46) Chen, Z.; Guan, Z.; Li, M.; Yang, Q.; Li, C. Enhancement of the performance of a platinum nanocatalyst confined within carbon nanotubes for asymmetric hydrogenation. *Angew. Chem., Int. Ed.* **2011**, *50*, 4913−4917.

(47) Huck, W.-R.; Mallat, T.; Baiker, A. Non-linear effect of modifier composition on enantioselectivity in asymmetric hydrogenation over platinum metals. *Adv. Synth. Catal.* **2003**, *345*, 255−260.

(48) Bartók, M.; Felföldi, K.; Szöllösi, G.; Bartók, T. Rigid cinchona conformers in enantioselective catalytic reactions: New cinchona-modified platinum catalysts in the orito reaction. *Catal. Lett.* **1999**, *61*, 1−5.

(49) Lou, L.-L.; Yang, T.; Yu, W.; Qu, H.; Feng, Y.; Li, H.; Yu, K.; Liu, S. Effective and durable Pt nanocatalyst supported on three-dimensionally ordered macroporous carbon for asymmetric hydrogenation. *Catal. Today* **2017**, *298*, 197−202.

(50) Blaser, H.-U.; Jalett, H.-P.; Garland, M.; Studer, M.; Thies, H.; Wirth-Tijani, A. Kinetic studies of the enantioselective hydrogenation of ethyl pyruvate catalyzed by a cinchona modified Pt/Al$_2$O$_3$ catalyst. *J. Catal.* **1998**, *173*, 282−294.

(51) Zuo, X.; Liu, H.; Liu, M. Asymmetric hydrogenation of α-ketoesters over finely dispersed polymer-stabilized platinum clusters. *Tetrahedron Lett.* **1998**, *39*, 1941−1944.

(52) Zuo, X.; Liu, H.; Guo, D.; Yang, X. Enantioselective hydrogenation of pyruvates over polymer-stabilized and supported platinum nanoclusters. *Tetrahedron* **1999**, *55*, 7787−7804.

(53) Corro, G.; Fierro, J. L. G.; Odilon, V. C. An XPS evidence of Pt^{4+} present on sulfated Pt/Al$_2$O$_3$ and its effect on propane combustion. *Catal. Commun.* **2003**, *4*, 371−376.

(54) Song, A.; Lu, G. Enhancement of Pt-Ru catalytic activity for catalytic wet air oxidation of methylamine via tuning the Ru surface chemical state and dispersion by Pt addition. *RSC Adv.* **2014**, *4*, 15325−15331.

(55) Resende, N. S.; Perez, C. A.; Eon, J. G.; Schmal, M. The effect of coating TiO$_2$ on the CO oxidation of the Pt/gamma-alumina catalysts. *Catal. Lett.* **2011**, *141*, 1685−1692.

(56) Qiu, L.; Liu, F.; Zhao, L.; Yang, W.; Yao, J. Evidence of a unique electron donor-acceptor property for platinum nanoparticles as studied by XPS. *Langmuir* **2006**, *22*, 4480−4482.

(57) Fu, X.; Wang, Y.; Wu, N.; Gui, L.; Tang, Y. Surface modification of small platinum nanoclusters with alkylamine and alkylthiol: An XPS study on the influence of organic ligands on the Pt 4f binding energies of small platinum nanoclusters. *J. Colloid Interface Sci.* **2001**, *243*, 326−330.

(58) Kale, M. J.; Christopher, P. Utilizing quantitative in situ FTIR spectroscopy to identify well-coordinated Pt atoms as the active site for CO oxidation on Al$_2$O$_3$-supported Pt catalysts. *ACS Catal.* **2016**, *6*, 5599−5609.

(59) Hayden, B. E.; Kretzschmar, K.; Bradshaw, A. M.; Greenler, R. G. An infrared study of the adsorption of CO on a stepped platinum surface. *Surf. Sci.* **1985**, *149*, 394−406.

(60) Ye, J.-Y.; Attard, G. A.; Brew, A.; Zhou, Z.-Y.; Sun, S.-G.; Morgan, D. J.; Willock, D. J. Explicit detection of the mechanism of platinum nanoparticle shape control by polyvinylpyrrolidone. *J. Phys. Chem. C* **2016**, *120*, 7532−7542.

(61) Attard, G. A.; Bennett, J. A.; Mikheenko, I.; Jenkins, P.; Guan, S.; Macaskie, L. E.; Wood, J.; Wain, A. J. Semi-hydrogenation of alkynes at single crystal, nanoparticle and biogenic nanoparticle surfaces: The role of defects in Lindlar-type catalysts and the origin of their selectivity. *Faraday Discuss.* **2013**, *162*, 57−75.

(62) Campisi, S.; Ferri, D.; Villa, A.; Wang, W.; Wang, D.; Kröcher, O.; Prati, L. Selectivity control in palladium-catalyzed alcohol oxidation through selective blocking of active sites. *J. Phys. Chem. C* **2016**, *120*, 14027−14033.